

Review

Not peer-reviewed version

---

# False Liver Metastasis by PET/CT Scan After Chemoradiotherapy for Esophageal Cancer- A Potential Overstaged Pitfalls of Treatment

---

[Sen-Ei Shai](#)\*, [Yi-Ling Lai](#), [Chen-I Chang](#), Chi-Wei Hsieh

Posted Date: 23 January 2024

doi: 10.20944/preprints202401.1684.v1

Keywords: False Liver Metastasis; neoadjuvant chemoradiotherapy (nCRT); F-18-fluorodeoxyglucose (18F-FDG); positron emission tomography computed tomography (PET-CT); radiation-induced liver injury (RILI); radiation-induced liver disease (RILD)



Preprints.org is a free multidiscipline platform providing preprint service that is dedicated to making early versions of research outputs permanently available and citable. Preprints posted at Preprints.org appear in Web of Science, Crossref, Google Scholar, Scilit, Europe PMC.

Copyright: This is an open access article distributed under the Creative Commons Attribution License which permits unrestricted use, distribution, and reproduction in any medium, provided the original work is properly cited.

*Systemic Review*

# False Liver Metastasis by PET/CT Scan After Chemoradiotherapy for Esophageal Cancer—A Potential Overstaged Pitfalls of Treatment

Sen-Ei Shai <sup>1,2,3,\*†</sup>, Yi-Ling Lai <sup>1,†</sup>, Chen-I Chang <sup>4</sup> and Chi-Wei Hsieh <sup>5</sup>

<sup>1</sup> Department of Thoracic Surgery, Taichung Veterans General Hospital, Taichung, 40705, Taiwan; sse50@yahoo.com

<sup>2</sup> Department of Applied Chemistry, National Chi Nan University, Nantou, 545301, Taiwan; sse50@yahoo.com

<sup>3</sup> Institute of Clinical Medicine, National Yang-Ming Chiao-Tung University, Taipei, 112304, Taiwan; sse50@yahoo.com

<sup>4</sup> School of Medicine, National Yang-Ming Chiao-Tung University, Taipei, 112304, Taiwan; jenny28950@gmail.com

<sup>5</sup> School of Medicine, National Cheng Kung University, Tainan 701401, Taiwan; peter100yahoo@gmail.com

\* Correspondence: sse50@yahoo.com; Tel.: +886-975351109

† These authors contributed equally to this work.

**Simple Summary:** FDG PET-CT scans are critical in detecting metastases during neoadjuvant chemoradiotherapy for esophageal cancer, particularly for potential liver involvement. The liver's proximity to the radiation field in distal esophageal cancer therapies raises the risk of radiation-induced liver damage. Therefore, greater FDG absorption in the liver does not always imply metastases; it could also signal radiation-induced damage, which is a concern for distal esophageal carcinoma therapies in the left hepatic lobe, potentially leading to overstaging. Accordingly, thorough monitoring of FDG activity in the liver is required to reliably distinguish between radiation effects and genuine distant metastases. If FDG activity is seen in the left or caudate liver lobes following CRT, additional diagnostic procedures are demanded to confirm or rule out distant metastases. Surgery, usually scheduled 6-8 weeks after CRT, should be followed by a PET-CT scan to look for new interval metastases, as their existence may prohibit surgical intervention.

**Abstract:** For esophageal cancer patients treated with neoadjuvant chemoradiotherapy (nCRT), restaging using F-18-fluorodeoxyglucose (18F-FDG) positron emission tomography computed tomography (PET-CT) following nCRT can detect interval metastases, including liver metastases, in almost 10% of patients. However, in clinical practice, focal FDG liver uptake, unrelated to liver metastases, is observed after chemoradiotherapy. This radiation-induced liver injury (RILI) can potentially lead to overstaging. Liver radiation damage is also a concern during distal esophageal cancer radiotherapy due to proximity to the left liver lobe, typically included in the radiation field. Post-CRT, if FDG activity appears in the left or caudate liver lobes, thorough investigation is needed to confirm or rule out distant metastases. The increased FDG uptake in liver lobes post-CRT often presents a diagnostic dilemma. Distinguishing between radiation-induced liver disease and metastasis is vital for appropriate patient management, necessitating a combination of imaging techniques and an understanding of the factors influencing radiation response. Diagnosis involves identifying new foci of hepatic FDG avidity on PET/CT scans. Geographic regions of hypoattenuation on CT and well-demarcated regions with specific enhancement patterns on contrast-enhanced CT scan and MRI are characteristic of radiation-induced liver disease (RILD). Lack of mass effect on all three modalities (CT, MRI, PET) indicates RILD. Resolution of abnormalities on subsequent examinations also helps in diagnosing RILD. Moreover, it can also help to rule out occult metastases, thereby excluding those patients from further surgery who will not benefit from esophagectomy with curative intent.

**Keywords:** False Liver Metastasis; neoadjuvant chemoradiotherapy (nCRT); F-18-fluorodeoxyglucose (18F-FDG); positron emission tomography computed tomography (PET-CT); radiation-induced liver injury (RILI); radiation-induced liver disease (RILD)

## 1. Introduction

Esophageal cancer causes death over 450,000 people each year and is the sixth leading cause of cancer-related death globally.<sup>[1]</sup> Currently, surgical resection of the esophagus preceded by neoadjuvant chemoradiotherapy (nCRT) is the standard of treatment for patients with non-metastasized esophageal cancer.<sup>[1-3]</sup> nCRT results in downstaging of the tumor, increases the radical resection rate, and is associated with a survival benefit.<sup>[2, 3]</sup> Esophageal cancer often metastasizes to the abdomen's lymph nodes, liver, and lungs<sup>[4]</sup>, with liver metastases developing in up to 35% of cases.<sup>[5]</sup> Several small studies have assessed the role of F-18-fluorodeoxyglucose (18F-FDG) positron emission tomography computed tomography (PET-CT) for pre-surgical restaging after neoadjuvant therapy, with reported incidence rates of interval metastases varying from 2% up to 26%.<sup>[6, 7]</sup> However, most studies did not report diagnostic accuracy measures (i.e. sensitivity, specificity) and included only a small number of patients.<sup>[8-10]</sup> Accurate preoperative detection of (interval) metastasis of esophageal cancer is crucial for optimal selection of patients suitable for surgery.<sup>[11]</sup> The liver's radiosensitivity has historically constrained radiation therapy for liver and upper abdominal perihepatic tumors.<sup>[12]</sup> Nevertheless, radiation damage to the liver, particularly its lateral segment near the distal esophagus, is hard to prevent.<sup>[13]</sup> Preoperative whole-body PET-CT is common for assessing radiation response and ruling out metastases. PET-CT can detect radiation-induced liver damage 2 to 6 weeks post-therapy, evident as increased FDG uptake (>50% above baseline) near the irradiated area, accompanied by reduced CT attenuation.<sup>[13]</sup> Radiation-induced liver disease (RILD), a significant concern post-radiation, can manifest as either classic or non-classic types. RILD, previously termed radiation hepatitis, can cause both diffuse as well as focally increased FDG uptake on PET-CT.<sup>[14]</sup> Understanding its pathophysiology, including factors like retrograde congestion and the role of key cytokines, is crucial for early detection and management.<sup>[15-20]</sup> Although PET-CT is effective in assessing response of the primary tumor to nCRT and has the ability to identify interval metastases, the effectiveness of PET-CT in accurately identifying metastatic disease, as well as the implications associated with false-positive PET-CT findings with regard to the sites of false-positive results and the subsequent work-up to investigate them, are much less described.<sup>[21]</sup> There appeared to be no association between the response of the primary esophageal tumor to nCRT and the detection of interval metastases. In the patients with true interval metastases, none mostly were found to have progressive or enlarging disease of the primary.<sup>[21]</sup> No pre-therapy metastasis signs were seen, but a new FDG lesion emerged during restaging. This lesion could result from chemotherapy, radiation, or their combination.<sup>[9, 10, 22]</sup> Risks of RILD increase with concurrent hepatotoxic chemotherapy.<sup>[16]</sup> Liver radiation tolerance decreases in patients with impaired liver function, increasing their RILD risk.<sup>[16]</sup> This structured approach will guide through the complexities of diagnosing and managing false simulations of liver metastasis in esophageal cancer patients post-nCRT.

## 2. Mechanism and Application of PET-CT Scan

### 2.1. Imaging Principles and Clinical Application

FDG is a non-physiological analogue of glucose that varies only slightly from the chemical structure of the glucose molecule. It undergoes normal cellular transport and metabolic pathways.<sup>[23]</sup> Once injected, FDG is taken up by cell membrane glucose receptors (principally, the glucose transporter-1 molecule, GLUT-1) that transport it into the intracellular compartment, where it is phosphorylated into FDG-6-phosphate by the enzymatic action of hexokinase. The overall effect is that FDG becomes trapped in the cancer cell, failing to undergo further metabolism; consequently, this can be exploited to visualize the metabolic activity at sites of tumoral involvement. However, it has long been recognized that active benign pathological conditions, such as inflammatory and infective processes, may also show increased accumulation of FDG. This is largely due to the enhanced glycolytic metabolism that accompanies inflammatory cellular infiltrates, incorporating activated macrophages, monocytes, and polymorphonuclear cells, which are all actively involved in the recruitment, activation, and healing phases of tissue inflammation.<sup>[24]</sup>

Integrated PET-CT using the glucose analogue 18F-FDG is established in the imaging procedures of oncological patients. The recognition that combined metabolic and morphological information yielded by PET-CT can have a significant impact on tumor staging and restaging, detection of recurrent disease and optimization of therapy in a wide variety of solid-organ malignancies, along with increased access to this imaging technique, has led to greater utilization of PET-CT in oncological patients in recent years.<sup>[25-28]</sup> Role of PET-CT in preoperative evaluation for esophageal cancer was that preoperative whole-body PET/CT scans are instrumental in assessing the response to radiation treatment and ruling out metastases; meanwhile, detecting radiation-induced liver injury, characterized by increased FDG uptake in areas adjacent to the irradiated field, is crucial for accurate staging and treatment planning.<sup>[12, 13]</sup>

2.2. False positive and false negative PET/CT: Causes and Probabilities

2.2.1. Caveats in interpreting PET-CT in individuals with esophageal cancer in Table 2

**Table 1.** Caveats in the interpretation of PET-CT in patients with Esophageal cancer.

Causes of False-Positive Findings	Casuses of False-Negative Findings
Infections/Inflammatroy lesions	Lesion dependent
Radiation-induced liver disease (RILD)	Small tumors (<8-10 mm)
Radiation pneumonitis	Low metabolic activity of the tumor
(Postobstructive) pneumonia/abscess	The presence of a treatment-induced decrease in tumor metabolism
Mycobacterial or fungal infection	Technique limitation
Granulomatous disorders (sarcoidosis, Wegener)	Hyperglycemia
Chronic nonspecific lymphadenitis	Paravenous FDG injection
(Rheumatoid) arthritis	Excessive time between injection and scanning
Occupational exposure (anthracosilicosis)	Low resolution or motion artifacts
Bronchiectasis	
Organizing pneumonia	
Reflux esophagitis	
Iatrogenic causes	
Invasive procedure (puncture, biopsy)	
Talc pleurodesis	
Radiation esophagitis and pneumonitis	
Bone marrow expansion postchemotherapy	
Colony-stimulating factors	
Thymic hyperplasia postchemotherapy	
Benign mass lesions	
Salivary gland adenoma (Whartin)	
Thyroid adenoma	
Adrenal adenoma	
Colorectal dysplastic polyps	
Focal physiological FDG uptake	
Gastrointestinal tract	
Muscle activity	
Brown fat	
Unilateral vocal cord activity	
Artherosclerotic plaques	

2.2.3. Common non-malignant pathological conditions showing increased uptake of FDG before therapy

It has been estimated that benign non-physiological lesions with increased uptake of FDG are encountered in more than 25% of PET-CT studies performed in oncological patients.<sup>[29-31]</sup> Detection of malignant infiltration of lymph nodes is an important requirement in the accurate staging of most cancers, and FDG PET-CT can make a significant contribution to this process by demonstrating tumor involvement in non-pathologically enlarged nodes. However, there are numerous causes of false-positive nodal uptake of FDG. These include inflammatory causes, such as sarcoidosis or sarcoid-like reaction to malignancy, collagen-vascular diseases and anthracosis, and infective causes such as TB, infectious mononucleosis, acquired immunodeficiency syndrome (AIDS), and hepatitis C.<sup>[32, 33]</sup>

3. Current Treatment Protocol of Esophageal Cancer Involving True Liver Metastasis and False Liver Metastasis

3.1. Current Standard Procedure of Treatment for Esophageal Cancer in Figure 1

The typical duration between the completion of nCRT and esophagectomy can vary depending on the specific treatment protocol and the patient's response to nCRT. Generally, a waiting period of about 4 to 8 weeks is considered to allow the patient to recover from the effects of chemoradiation and for any potential downsizing or downstaging of the tumor to occur. This period also allows for the assessment of the patient's fitness for surgery and for any necessary preoperative planning.

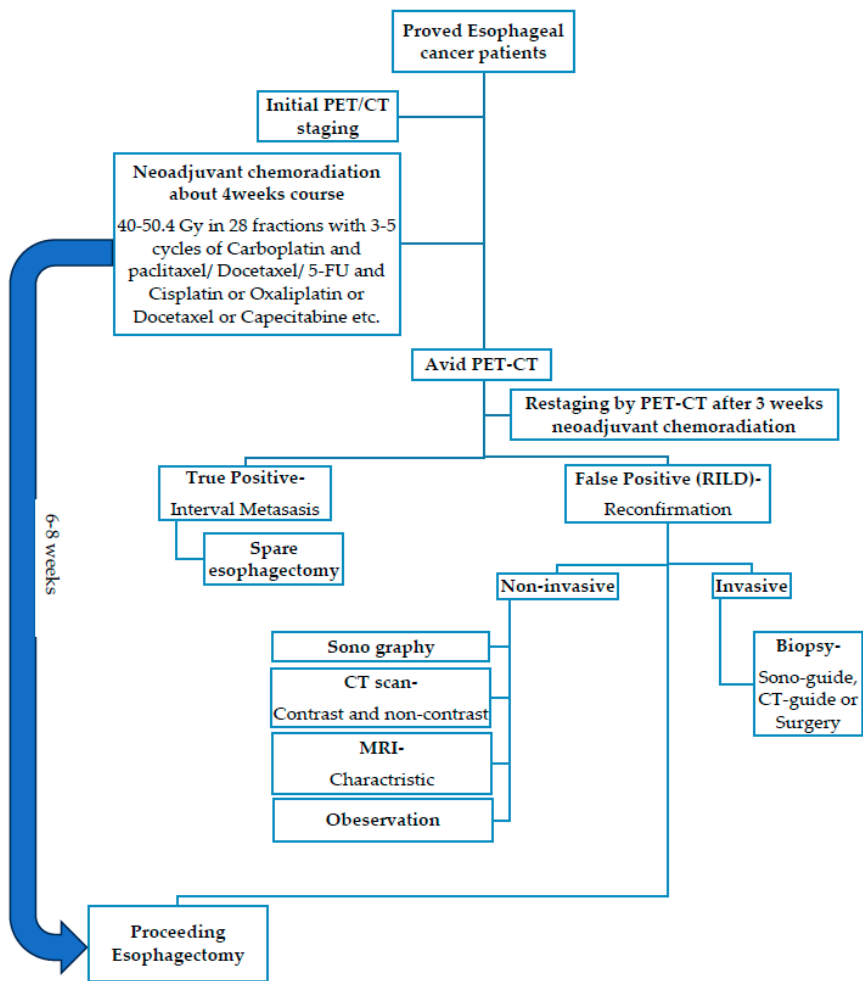


**Figure 1.** Schematic figure of current gold standard procedure for esophageal cancer treatment with nCRT followed by esophagectomy.



NCRT for locally advanced esophageal cancer is accepted practice prior to surgical resection, as supported by the Chemoradiation for esophageal Cancer Followed by Surgery Study (CROSS) trial.<sup>[34]</sup> Restaging imaging is recommended to ensure that interval progression of disease or new metastases has not developed which would deem the patient unresectable.<sup>[35]</sup> In esophageal carcinoma, neo-adjuvant radiotherapy can be administered by three-dimensional (3D) conformal therapy or intensity-modulated therapy (IMRT). The application of IMRT results in a net increase of radiation dose to the primary tumor while limiting damage to surrounding tissue, when compared to conventional anterior–posterior opposing field radiotherapy.<sup>[13]</sup> At restaging with FDG-PET-CT after chemoradiotherapy, 8% of patients are found to have interval metastases.<sup>[9, 10]</sup> However, inflammatory reactions may induce false-positive results on FDG-PET-CT.<sup>[36, 37]</sup> Radiation-induced liver injury is described in 3–8% of patients who are reassessed with a PET-CT scan after neoadjuvant CRT. Although this phenomenon is relatively rare, awareness of its existence is important to prevent a false positive diagnosis of metastatic disease (**Table 3**).<sup>[14]</sup>

**Table 3.** Diagnostic parameters of 18F-FDG PET-CT for the detection of interval metastasis.<sup>[11]</sup>

Parameter	18F-FDG PET-CT
Sensitivity (%) [95%CI]	65/87 (74.7%) [64.3–83.4]
Specificity (%) [95%CI]	652/696 (93.7%) [91.6–95.4]
Positive predictive value (%) [95%CI]	65/109 (59.6%) [52.0–66.9]
Negative predictive value (%) [95%CI]	652/674 (96.7%) [95.4–97.7]
Diagnostic accuracy	91.6%

3.2. Reports of The Reference of True and False Metastasis for Restaging after nCRT

A retrospective analysis of 112 patients with distal esophageal cancer receiving nCRT and restaging PET-CT found new liver foci in 10/112 patients (9%). Nine of these were determined to have radiation-induced liver injury based on further imaging (n = 6) or biopsy (n = 2) and 1 patient had developed interval metastatic disease based on biopsy. Radiation-induced liver injury was solely seen in the caudate and left hepatic lobes.<sup>[22]</sup> Another retrospective study of 26 patients evaluated FDG uptake in the liver before and after nCRT for esophageal cancer. New focal FDG uptake in the left liver lobe after chemoradiation was seen in 2 patients (8%) with no increase of FDG in the right part of the liver. In one of these patients, biopsy confirmed radiation injury. On CT, atrophy and decreased attenuation of the irradiated left liver lobe were found in 58% of patients, without signs of liver metastases.<sup>[13]</sup>

3.2.1. Case Reports Series and Cohort Study

The results of the present study indicate that (interval) metastases are detectable in more than 10% of esophageal cancer patients who receive nCRT. With a sensitivity and specificity of 73.9% and 91.3% respectively, PET-CT is an accurate tool to identify these cases. Currently an unequivocal restaging protocol is still absent, even though previous reports on this topic have shown incidence rates of interval metastases between 8%-17%.<sup>[8, 38-41]</sup> Presently, two reports have addressed the use of PET-CT in detection of interval metastases as a primary topic. In a recent study by Blom et al. 4 cases of interval metastases were detected in a consecutive series of 50 neoadjuvantly treated patients (8%).<sup>[8]</sup> Restaging PET-CT took place 6 weeks after completion of neoadjuvant therapy that consisted of 5-FU, cisplatin and 50.4 Gy radiotherapy. A false-positive rate of 2% was reported in this cohort and in 1 out of 46 patients (2.2%) metastatic disease was observed intraoperatively.<sup>[8]</sup> In another study on restaging PET-CT the records of 85 patients treated either with induction chemotherapy followed by concurrent chemoradiotherapy or with concurrent chemoradiotherapy only were retrospectively reviewed.<sup>[38]</sup> In all patients who underwent a pre-nCRT PET-CT, the post-nCRT PET-CT identified metastatic disease in only 3.9% of patients. The PPV of the post-nCRT PET-CT for interval metastases

was low at 15.6% (10/64). Regardless of the cause for this observation, post-nCRT PET-CT findings pertaining to the primary site did not seem to be related to the development of metastatic disease.<sup>[21]</sup>

Findings in the current study demonstrate that 18F-FDG PET-CT restaging after nCRT detects interval metastases in 8% of esophageal cancer patients, with a patient-based sensitivity and specificity of 75% and 94%, respectively. The incidence of interval metastasis in the current study is consistent with the results of previous reports.<sup>[8-10]</sup> Yet, little is known about what patients are at risk for developing interval metastases, and the small number of patients in the previous mentioned studies precludes assessment of predictors for interval metastasis after neoadjuvant therapy.<sup>[8-10, 42]</sup> the false positive rate of 6% during 18F-FDG PET-CT restaging was substantial, with the lungs and liver as the most frequent affected sites. This confirms previous findings in literature, with reported false positive rates ranging between 0% and 10%<sup>[8, 43]</sup> and liver and lung as the most commonly affected sites.<sup>[21, 22]</sup> Previous studies evaluating new FDG-avid hepatic lesions within the presumed radiation field of patients with esophageal cancer demonstrated that these lesions generally reflect radiation-induced liver disease rather than metastatic disease.<sup>[13, 14, 22]</sup> 18F-FDG PET-CT restaging detects true distant interval metastases in 8.3% of patients after chemoradiotherapy for esophageal cancer.<sup>[11]</sup>

Table 4. Review of current case reports by Demey et al., 2017<sup>[44]</sup>.

Table 4. Overview of current case reports.											
Author (Year)	Age	TNM-pathology	Chemotherapy	Radiotherapy dose-Modality	Delay CRT to PET	PET	CT	MR	Biopsy	Liver Tests	Follow-up
Iyer et al.[2] (2007)	63	NA- adeno	NA	50.4 Gy - 3D conformal	6w	Nodular	Well-defined, low attenuation	-	Pero p	AP↑	NA
Iyer et al.[2] (2007)	NA	NA- NA	NA	50.4 Gy - 3D conformal	6w	Nodular	Well-defined, low attenuation	-	NA	AP↑	NA
Nakahara et al.[3] (2008)	50	uT3N M2 1(bone ) - NA	Docetaxel weekly (20mg/m2 )	46 Gy + boost 14 Gy - AP- RT	4w	Wedge-shaped	Well-defined, low attenuation + band-likelesion (≈zoneof < 40Gy)	-	NA	AP↑	4months
DeLape et al.[5] (2009)	61	uT3N M1 0 - NA	4 cycli (apirubicine + oxaliplatin + capcetabine) + 3 cycli (docetaxel + irinotecan ) + concurrent 5-FU	50.4 Gy - IMRT	5w	Ill-defined nodular	Patchy defined, mixed attenuation, heterogeneous enhancement of left liver	-	CT-guided + perop	NA	NA
Wong et al.[6] (2012)	58	NA - NA	NA	50.4 Gy - AP-RT	6w	Nodular with linear distribution	Patchy-defined, low attenuation in segment 2 and 3	-	NA	Normal	NA

Rabe et al.[8] (2015)	53	uT3N M1 0 - squamous	5 cyclin (carboplatin + paclitaxel)	50.4 Gy - 3D conformal	2w	Nodular	Well-defined, low attenuation	Hyperintense T2-weighted	Pero p	AP↑	12months
Current case (2015)	42	uT2N M1 0 - adeno	Concurrent Oxaliplatin + 5-FU	45 Gy - 3D conformal	4w	Nodular	Patchy-defined, low attenuation in segment 2	Hyperintense T2-weighted	Pero p	Normal	18months

NA: data not available; adeno: adenocarcinoma; Gy: Gray; w: weeks; AP "": elevated alkaline phosphatase levels; AP-RT: conventional anterior-posterior radiotherapy; IMRT: intensity-modulated radiation therapy; 5-FU: 5-fluorouracil.

4. RILD Inducing False PET-CT

Clinical radiation injury in the left liver lobe, given its anatomical location, may occur in 6–66% of patients depending on the volume of hepatic tissue irradiated and the dose used.<sup>[13]</sup> Grant et al. found that all new 18FDG-PET-CT lesions in the right lobe were metastatic, comparing to the lesions in the left or caudate lobe that were all radiation-induced injuries. The radiation fields should therefore carefully be compared with the location of the nodular lesion and only lesions outside the field should be considered highly suspicious of metastases.<sup>[22]</sup> Preoperative 18F-FDG-PET-CT is useful in the reevaluation after neo-adjuvant chemoradiotherapy to determine treatment response and exclude occult metastasis.<sup>[44]</sup> Eithne M. DeLappe reported a 61-year-old esophageal cancer patient with increased FDG uptake in the left liver lobe post-50.4Gy radiation, with no metastasis found in biopsy.<sup>[45]</sup> In Oregon, USA, 112 distal esophageal cancer patients underwent neo-adjuvant chemo-radiotherapy; ten showed increased FDG uptake during restaging, with one later diagnosed with metastasis, while others had radiation-induced liver injury.<sup>[22]</sup> At the Anderson Cancer Center, 26 esophageal cancer patients received similar treatment; two showed increased FDG uptake in the left liver lobe, with no uptake in the right.<sup>[13]</sup> In a study by Francine et al., involving 205 patients, six showed increased FDG uptake in the caudate or left lobe during nCRT, but none had liver metastasis.<sup>[14]</sup> Hepatic Radiosensitivity: The organ involvement in chemoradiation-induced injuries varies, with the lung, liver, heart, spinal cord, kidney, bowel, among others, being susceptible. The liver's sensitivity to radiation limits the use of radiation therapy for tumors in the upper abdomen.<sup>[12, 13]</sup>

4.1. Implications of Increased FDG Uptake

The mechanism of FDG accumulation in radiation-induced liver injury is uncertain; most likely it is caused by an inflammatory component. It is well known that (radiation-induced) inflammation, such as postradiotherapy esophagitis<sup>[36]</sup>, is FDG-avid due to high glucose uptake of leukocytes.<sup>[5, 46]</sup> The duration and timing of this phenomenon is also unclear. Acute side effects of chemoradiotherapy increase during and shortly after treatment. Thereafter, they slowly diminish, which may take 6 weeks or more. It would be interesting to follow-up patients suspected of RILI with serial PET-CT scans, to learn more about its natural course in time.<sup>[14]</sup> Frequency and appearance of RILD on PET-CT: A study found that new foci of FDG avidity developed in the liver during neoadjuvant therapy in 9% of patients, with 8% determined to have RILD based on further imaging and/or biopsy.<sup>[22]</sup> Common sites of metastasis in esophageal cancer include liver, and both metastases and RILD may manifest as increased FDG avidity. The study highlighted that new hepatic FDG avidity during neoadjuvant chemoradiation is usually due to RILD, not metastasis.<sup>[22]</sup> NCRT for esophageal cancer can lead to liver damage, mimicking liver metastasis on PET-CT. This damage commonly appears in the caudate and left hepatic lobes.<sup>[47]</sup> RILD may be detected by PET-CT as a focal area of increased FDG uptake, often confused with metastatic disease.<sup>[47]</sup>

4.2. The Formation and Classification of RILD



RILD exists in two forms: classic and non-classic.<sup>[17]</sup> Classic RILD symptoms, appearing 1–3 months post-liver RT, include fatigue, abdominal pain, increased girth, hepatomegaly, and anicteric ascites.<sup>[18]</sup> Non-classic RILD patients, often with chronic liver conditions like cirrhosis or viral hepatitis, show more severe hepatic dysfunctions, including jaundice and high serum transaminases.<sup>[17]</sup> Radiotherapy to the distal esophagus and locoregional nodes can result in a substantial dose to the adjacent nonmalignant hepatic parenchyma, which can result in acute or chronic radiation hepatitis (RH).<sup>[5, 13]</sup> RH can be seen on CT as atrophy and attenuation changes of the liver, and PET/CT may identify metabolic abnormalities in the irradiated liver parenchyma.<sup>[13]</sup> but RILD's exact development mechanisms are largely unknown.<sup>[17]</sup> Radiation damage likely starts with central vein and sinusoid endothelial cell damage, causing sinusoidal congestion and, in advanced stages, veno-occlusive disease leading to congestion and liver necrosis.<sup>[48, 49]</sup> Its hallmark is hepatic Veno Occlusive Disease (VOD), marked by central vein lumina blockage with erythrocytes in reticulin and collagen networks.<sup>[15, 19]</sup>

#### 4.3. Occurrence and Duration of RILD

Acute RH can occur in the liver after radiotherapy from a dose of 30 Gy onward. It usually appears 4–8 weeks after completion of the radiation therapy. On histopathology, acute RH is characterized by sinusoidal congestion and fibrously occluded central veins. Chronic RH appears more than 100 days post irradiation. It is characterized by portal fibrosis and distortion of lobular architecture whereas centrilobular congestion is not usually seen.<sup>[5, 50]</sup> RILD is characterized by symptoms like anicteric hepatomegaly, ascites, and elevated liver enzymes, typically occurring 2 weeks to 3 months after radiotherapy completion. Most patients recover in 3–5 months, but a minority may experience liver fibrosis and failure.<sup>[14]</sup> Reed and Cox initially described RILD's pathophysiology, identifying retrograde congestion as a primary factor.<sup>[15]</sup> RILD usually appears 4–8 weeks post-radiation but can emerge as early as 2 weeks or as late as 7 months.<sup>[16]</sup> About 8% of patients show radiation-induced liver injury (RILI) during restaging.<sup>[17]</sup>

#### 4.4. Incidence of RILD

In this systematic search of the reports, they found an incidence of RILI of 3%. Other retrospective reports found higher incidences (8%) of RILI when all scans were reassessed for focal uptake in the left liver lobe.<sup>[13, 22]</sup> A possible explanation for the lower incidence in this study is that some cases of RILI may have been missed by our systematic search. The risk of RILD increases strongly with the mean liver dose and the irradiated liver volume. After a mean liver dose <31 Gy, RILD is unlikely.<sup>[51, 52]</sup> In distal esophageal cancer, mean liver radiation doses are generally below 30 Gy. However, the radiation target volume often includes parts of the liver, which may receive doses up to 40–50 Gy. This can induce localized radiation induced injury in the liver without clinical symptoms.<sup>[5, 53, 54]</sup> In a study involving 205 patients undergoing nCRT, 6 cases with localized increased FDG uptake in the liver were identified post-nCRT. These cases were not associated with liver metastases. The incidence of RILD at the institute was 3%, and literature describes it as about 8% of patients at the time of restaging.<sup>[14]</sup>

##### 4.4.1. If Tumor Cell Type Pose Different Risk Factors for RILD: Squamous-Cell Carcinoma (SCC) and Adeno Carcinoma in Table 4

Distal esophageal cancers, including Squamous-Cell Carcinoma (SCC) and Adenocarcinoma, are associated with distinct risk factors. The table highlights alcohol consumption as a major risk factor for SCC. This suggests that patients with SCC might have a higher incidence of liver dysfunction compared to those with Adenocarcinoma, potentially increasing the likelihood of Radiation-Induced Liver Disease (RILD). However, this area remains underexplored in medical literature, indicating a need for additional research to understand these correlations better.

**Table 4.** Risk factors for esophageal cancer\* from Enzinger et al., 2003 [55]).

Risk Factor	Squamous-Cell Carcinoma	Adenocarcinoma
Tobacco use	+++	++
Alcohol use	+++	-
Barrett’s esophagus	-	++++
Weekly reflux symptoms	-	+++
Obesity	-	++
Poverty	++	-
Achalasia	+++	-
Caustic injury to the esophagus	++++	-
Nonepidermolytic palmoplantar keratoderma (tylosis)	++++	-
Plummer–Vinson syndrome	++++	-
History of head and neck cancer	++++	-
Frequent consumption of extremely hot beverages	+	-

\*A single plus sign indicates an increase in the risk by a factor of less than two, two plus signs an increase by a factor of two to four, three plus signs an increase by a factor of more than four to eight, and four plus signs an increase by a factor of more than eight. The plus–minus sign indicates that conflicting results have been reported, and the dashes indicate that there is no proven risk.

4.4.2. Gender, age, race

While it is known that esophageal cancer predominantly affects males, the specific sensitivities of different genders, ages, and ethnicities to Radiation-Induced Liver Disease (RILD) remain unclarified in existing literature. Currently, there is a lack of detailed statistical analysis on these aspects, highlighting a significant area for future research attention.

4.5. Molecule Biology of RILD

Recent advances in understanding RILD pathogenesis haven’t clarified its molecular pathways.[17] RILD's pathogenesis includes vascular changes, increased collagen synthesis, and activation of growth factors and cytokines like TNF- $\alpha$ , TGF- $\beta$ , and Hedgehog. These factors play a significant role in liver repair. [56] Radiation exposure leads to DNA damage, oxidative stress, and reactive oxygen species production, causing hepatocellular apoptosis and inflammatory responses. An interesting observation is the role of Kupffer cells (KCs) in increasing hepatocytes' susceptibility to radiation-induced apoptosis through TNF- $\alpha$  secretion. Hepatic stellate cells (HSCs) also play a pivotal role, as they are transdifferentiated into myofibroblastic HSCs, the main collagen-producing cells in the liver, upon radiation exposure. This transdifferentiation is crucial in the development of RILD due to the high radiosensitivity of these cells. Moreover, sinusoidal endothelial cell (SEC) apoptosis is identified as a primary event in radiation-induced liver damage.

RILD involves complex multicellular responses, including vascular changes, collagen synthesis, and activation of growth factors and cytokines like TNF- $\alpha$ , TGF- $\beta$ , and Hedgehog, key in liver repair.[56]

4.6. Influence of RILD

4.6.1. Dose of Radiotherapy

RILD radiation doses vary, with the literature mentioning pure doses up to 70 cGY, combined with 30 cGY chemotherapy, or adjusted doses for existing liver disease. The risk of RILD strongly correlates with the mean liver dose and the irradiated liver volume. In distal esophageal cancer, parts of the liver may receive doses up to 40-50 Gy, inducing localized RILD without clinical symptoms.[14] Various radiation doses and chemotherapy regimens were used in different cases, including 41.4 Gy, 50 Gy, and 50.4 Gy in combination with chemotherapy agents like carboplatin and cisplatin. [14]

#### 4.6.2. Synergic Effect with Chemotherapy

The cumulative effects of chemotherapy and radiotherapy, especially in cases using 3D conformal or IMRT, can lead to complex liver responses. Understanding the synergetic effects and liver's radiation tolerance is key to predicting and managing potential radiation-induced liver disease (RILD).<sup>[9, 10, 16, 22, 57, 58]</sup> No specific information was found in the provided documents.

#### 4.6.3. Underlying Liver Disease Is Vulnerable to RILD

No specific information was found in the provided documents regarding Hepatitis B or C virus infection, Liver cirrhosis, Hepatomegaly, and Liver function impairment. Hepatitis B virus carriers are more prone to RILD.<sup>[20]</sup> Hepatitis C is theorized to carry a similar risk level to Hepatitis B. Consequently, further exploration is warranted to better understand the implications for patients who have liver function risk factors linked to these hepatitis types.

### 4.7. Confirmation of RILD- Challenges in Characterizing RILD with Imaging

Differentiating RILD from metastatic disease using imaging techniques like PET/CT and MRI is fraught with challenges. Characteristic imaging features, though evolving, provide critical insights into the nature and extent of radiation-induced damage.<sup>[45, 53, 59-63]</sup> No specific information was found in the provided documents regarding Sono, CT, MRI, PET/CT liver sensitivity, or liver biopsy techniques.

#### 4.7.1. Sono of Liver and Its Sensitivity

Ultrasonography has been a mainstay for anatomical imaging of the liver. With the introduction of new techniques like elastography and quantitative ultrasound parameters, the capability to assess liver tissue properties beyond echogenicity has been enhanced. This includes the measurement of acoustic parameters to characterize tissue microstructure, which is promising for monitoring the severity of hepatic steatosis in chronic liver diseases. These advancements in ultrasound technology are significant for improving the sensitivity and specificity of liver disease diagnosis, particularly in the context of RILD.<sup>[64]</sup> Sonography of the liver reveals a hypoechoic appearance over the caudate lobe (**Figure 2A**).

#### 4.7.2. CT Scan and Its Sensitivity

Noninvasive imaging techniques for RILD characterization are evolving.<sup>[59]</sup> Post-radiotherapy CT scans of irradiated liver areas show reversible, distinct regions of reduced enhancement, possibly indicating increased water or fat.<sup>[53, 60, 61]</sup> Radiation-induced veno-occlusive disease can cause increased enhancement due to augmented arterial flow or delayed contrast clearance.<sup>[62]</sup> RILD may present as hypo or hyperattenuated non-anatomic areas<sup>[63]</sup>, with CT typically showing sharp, straight margins matching the radiation portals.<sup>[13]</sup> In contrast, metastatic lesions appear more mass-like and rounded on CT.<sup>[13]</sup> The CT-graphic appearance of acute RH has been described as areas of low attenuation with sharp linear borders on noncontrast CT, which can occur in patients who receive more than 30–45 Gy.<sup>[5, 12, 13, 65]</sup> Increased enhancement on contrast CT can be seen in the irradiated liver because increased arterial flow or delayed contrast clearance for radiation-induced veno-occlusive disease.<sup>[12]</sup> The contrast CT scan shows decreased enhancement in S1 of the liver (Figure 2B). Contrast-enhanced CT shows low attenuation due to edema at the irradiated area of the liver. Current advanced radiotherapy techniques using multiple beams from different angles have a less sharp dose gradient, with a relatively small volume of normal tissue close to the target volume receiving a relatively high dose, and a larger volume of surrounding tissue receiving lower doses. Liver injury is generally confined to the area irradiated to a high dose, resulting in focal areas of edema and lower attenuation on CT.<sup>[66]</sup>

#### 4.7.3. MRI and Its Sensitivity

MRI post-liver radiation reveals decreased T1 signal intensity, increased T2 intensity, and heightened proton spectroscopic imaging signals in irradiated lobes, suggesting increased water content.<sup>[61]</sup> MRI's high resolution and soft tissue contrast are ideal for organ differentiation.<sup>[67]</sup> Clinical studies use MRI to track radiation damage in the liver<sup>[68]</sup>, myocardium<sup>[69, 70]</sup>, and bone marrow.<sup>[71, 72]</sup> The MR of the liver was performed five weeks after radiation therapy, and showed a hypointense signal on T1-weighted images and strongly hyperintense signal on T2-weighted images and facilitated diffusion at DWI-images. Additionally, we saw heterogeneous alterations on T2-weighted and DWI-images of the entire left liver lobe, which was attributed to mild RH of this entire left liver lobe and central acute RH in segment 2.<sup>[44]</sup> MRI T1-weighted pictures of the liver reveal a low signal intensity over the caudate lobe (**Figure 2C**). MRI T2-weighted pictures of the liver indicate a strong signal intensity over the caudate lobe (**Figure 2D**). On magnetic resonance imaging (MRI), liver areas that received a high radiation dose generally have low signal intensity on T1-weighted images and high signal intensity on T2-weighted images, as a result of edema.<sup>[37, 66]</sup>

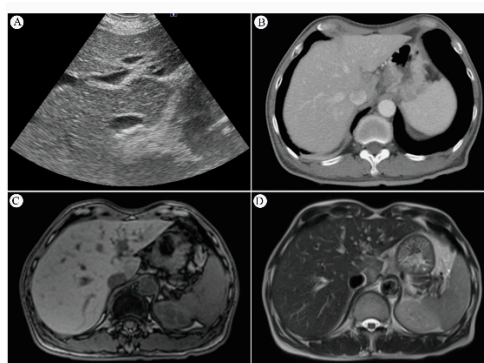


**Figure 2.** (A) Sonography of the liver reveals a hypoechoic appearance over the caudate lobe. (B) The contrast CT scan shows decreased enhancement in S1 of the liver. (C) MRI T1-weighted pictures of the liver reveal a low signal intensity over the caudate lobe. (D) MRI T2-weighted pictures of the liver indicate a strong signal intensity over the caudate lobe.

#### 4.7.4. SUVmax value of PET/CT Serve as Indicator of RILD?

Current studies lack comparisons of PET-CT SUVmax between radiation injury and metastatic lesions, but RILD SUVmax ranges around 4~9/h, while metastatic lesions often exceed 10/h, indicating metastasis. New hepatic FDG foci during esophageal cancer neoadjuvant chemoradiation typically indicate radiation-induced liver disease, with increased FDG uptake by active leukocytes due to inflammation.<sup>[45]</sup> This suggests a low metastasis likelihood.<sup>[22]</sup> Foci location within the radiation field, typically the left and caudate lobes, is crucial.<sup>[22]</sup> Prior to nCRT, the esophageal tumor exhibits high FDG uptake (9.7×5.6 cm, SUVmax: 29.3/1h) (red circles). There are no active lesions in liver segment I before nCRT (red arrows) (**Figure 3**). Shows esophageal tumor reduction after six weeks of neo-adjuvant chemo-radiotherapy (2.1×1.6 cm, SUVmax: 7.7/1h, highlighted in yellow circles) (**Figure 4**). Six weeks following neo-adjuvant chemo-radiotherapy, a new FDG-avid lesion was found in liver segment I (3.5×1.5 cm, SUVmax: 4.2/1h, indicated by yellow arrows) (**Figure 5**).

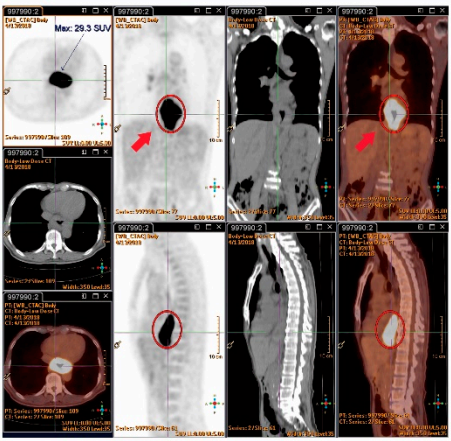


**Figure 3.** Prior to neoadjuvant chemoradiotherapy (nCRT), the esophageal tumor exhibits high FDG uptake (9.7×5.6 cm, SUVmax: 29.3/1h) (red circles). There are no active lesions in liver segment I before nCRT (red arrows).

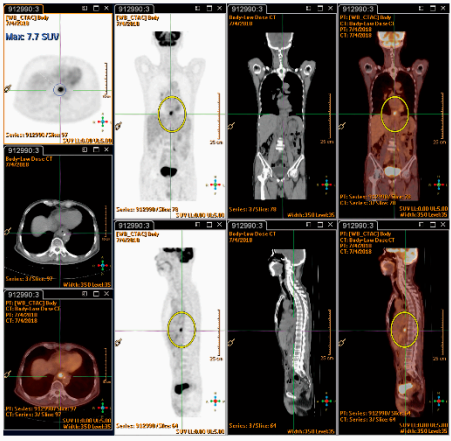


**Figure 4.** Shows esophageal tumor reduction after six weeks of nCRT (2.1×1.6 cm, SUVmax: 7.7/1h, highlighted in yellow circles).

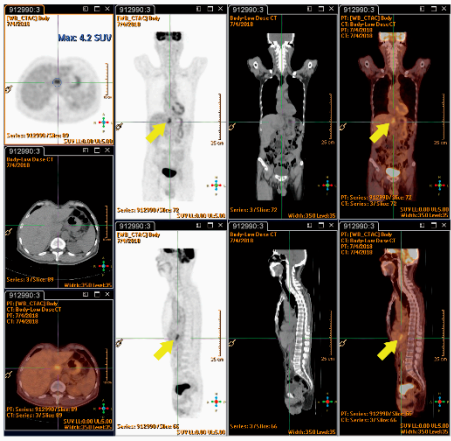


**Figure 5.** Six weeks following nCRT, a new FDG-avid lesion was found in liver segment I (3.5×1.5 cm, SUVmax: 4.2/1h, indicated by yellow arrows).



4.7.5. Biopsy for Diagnosis of Liver- Options by Sono-guiding, CT-guiding, Open biopsy or Clinical Observation

4.7.5.1. Pathology of RILD

RILD is a veno-occlusive disease involving the central veins.<sup>[49]</sup> Radiation-induced endothelial damage results in platelet activation, fibrin deposition, congestion of vessels, hepatic stellate cell activation, and blood flow obstruction, causing loss of hepatocytes, fibrosis, and even necrosis.<sup>[49]</sup>

4.7.5.2. Gross Appearance and Microscopy of RILD

The gross appearance and microscopic characteristics of RILD indicated significant pathological changes. The dark red, soft tissue, and blood infiltration in the caudate lobe suggest acute damage, likely due to the effects of radiation (Figure 6A-B). This is further supported by the microscopic findings of congestion with attenuated hepatic cords and spaces filled with erythrocytes (Figure 6C-D). These features typically point to a disruption in the normal liver architecture, indicating severe damage to the liver parenchyma, which could be attributed to the vascular and cellular effects of radiation exposure. This kind of damage often leads to impaired liver function due to the disruption of normal blood flow and cell death. The specific mention of the caudate lobe might also indicate a localized effect of radiation, which could be relevant for understanding the distribution and intensity of the radiation exposure.

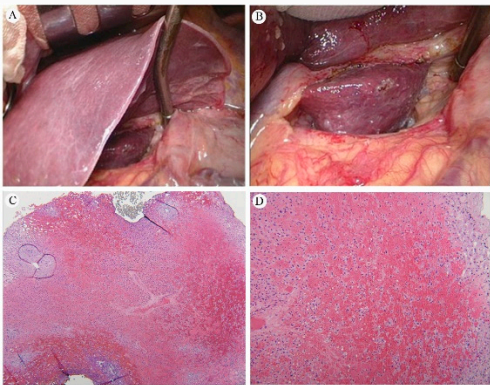


**Figure 6.** (A) The normal liver versus the inflamed caudate lobe. (B) An up-close image of the liver, showing dark red, soft tissue, and blood infiltration in the caudate lobe. Pathology of the liver caudate lobe. (C) A low-power field reveals no tumor metastasis at a magnification of 20X. (D) High power field indicates congestion with attenuated hepatic cords and filled with erythrocytes at a magnification of 40X.

5. Overview of Literature Review

	Auth or  (Year)	Gen der	Age (Range)	Race	Chemoradiotherapy			Liver functi on*	Stage	Esophageal cancer		
					Neoadj uvant	Dose	Medicine			SCC	Ade	Other
1	Rabe et al.  (2016)  [12]	F	53	NA	Yes	50.4Gy	Carboplatin and paclitaxel	Yes	T3N1M0- ->T2- weighted	1	0	0
2	Iyer et al.  (2007)	24M /2F	54 (41- 78)	NA	Yes	50.4 Gy/ patient	NA	Yes	NA	2	24	0

[10][13]												
3	Daly et al. (2007) [11]	74.2 %M /25.8 %F, n=50 44	67.3	76.8% Non-Hispani c Caucasian, 19.2% African America n, 4.0% Hispani c	NA	NA	NA	NA	Clinical stage - 0 (2.2%), I (14.1%), II (23.0%), III (22.1%), IV (38.7%).	51.6 0%	41.9 0%	0
4	Nakahara et al. (2008) [12]	M	50	NA	Yes	Up to a total of 46 Gy with an additional boost irradiation of 14 Gy.	Docetaxel	Yes	diagnosed with esophageal cancer with lymph node and bone metastases	NA	NA	0
5	Voncken et al. (2018) [13]	M	50	NA	Yes	50.4 Gy in 23 fractions with weekly carboplatin and paclitaxel	Carboplatin and paclitaxel	NA	T3N1M0	1	0	0
		M	62	Not specified	Yes	41.4 Gy in 23 fractions with weekly carboplatin and paclitaxel	carboplatin and paclitaxel	N0	T3N0M0	0	62	0
		M	41	NA	Yes	41.4 Gy in 23 fractions with weekly carboplatin and paclitaxel	Carboplatin and paclitaxel	No	T3N1M0	0	41	0
		M	59	NA	Yes	50 Gy	Cisplatin and 5-fluorouracil	No	T3N1M0	0	1	0
		M	49	NA	Yes	41.4 Gy	Carboplatin and paclitaxel	No	T3N1M0	0	1	0

6	Stieke ma et al. (2014) [6]	60M /16F	63 (46- 80)	NA	Yes	50 Gy or 50/ 50.4 Gy	5-FU/cisplatin or carboplatin and paclitaxel	NA	NA	14	60	2  (Undifferent iated)
		24M /2F	63 (46- 80)	NA	Yes	50 Gy (n= 21) or 41.4 Gy (n=50) or 50.4 Gy (n=5)	5-FU/cisplatin (n=21) or carboplatin and paclitaxel (n= 55)	NA	NA	9	39	
7	Grant et al. (2014) [14]	93M /19F	57 (28- 81)	NA	Yes	41.4-50.4 Gy	NA	NA	NA	21	97	4
8	Wied er et al. (2004) [15]	27M /11F	60 (46- 73)	NA	Yes	40 Gy	Fluorouracil	NA	NA	38	0	0
1 7	DeLa ppe et al. (2009) [41]	M	61	NA	Yes	50.4Gy	NA	NA	T3N1M0	0	1	0
1 8	Shai et al. (2020) []	M	66	Asian	Yes	5000cGy	NA	No	T3N1M0	1	0	0
1 9	Deme y et al. (2016)	M	42	NA	Yes	45Gy	Oxaliplatin, levofolinic acid and 5-FU	No	uT2N1M 0	0	1	0
2 0	Ander egg et al. (2015)	76.3 %M, n=15 6	65 (34- 83)	NA	Yes	41.4 Gy	Carboplatin and paclitaxel (n=139) or Cbp, Ptx and panitumumab (n=17)	NA	NA	29	126	1
2 1	Vonck en et al. (2018)	M	50	NA	Yes	50.4 Gy	Cbp and Ptx	NA	T3N1M0	1	0	0
		M	62	NA	Yes	41.4 Gy	Cbp and Ptx	No	T3N0M0	0	1	0

		M	41	NA	Yes	41.4 Gy	Carboplatin and Ptx	No	T3N1M0	0	1	0
		M	59	NA	Yes	50 Gy	Cis and 5-FU	No	T3N1M0	0	1	0
		M	49	NA	Yes	41.4 Gy	Cbp and Ptx	No	T3N1M0	0	1	0
		M	75	NA	Yes	50 Gy	Carboplatin/ etoposide	No	T2N1M0	0	0	1
2	Goens	675	<65	NA	Yes	45 Gy or 50.4 Gy	Oxaliplatin / 5- FU or Docetaxel / 5- FU or Capecitabine / 5-FU or other	NA	NA	111	672	0
2	e et al. (2018)	M /108F	(n=425), ≥65 (n=358)									
2	Gabri	234	61.5	NA	Yes	50.4 Gy	Cis and Iri/ Cbp and Ptx or Oxaliplatin/cap ecitabine or 5- FU and Cis	NA	NA	39	219	0
3	el et al. (2017)	M /24F										
2	Yueka	76M	56 (25- 82)	NA	NA	NA	NA	NA	NA	20	69	35
4	i et al. (2020)	/48F										
2	Blom	40	61 (56- 67)	NA	Yes	50.4 Gy	Cis and 5-FU	NA	Stages II to IVa	9	40	1
5	et al. (2011)	male / 10 fema le, n=50										
2	Cerfol	41	68 (48- 76)	NA	Yes	<50Gy (n=22), >50Gy (n=26)	NA	NA	Stages I to Ivb	5	43	0
6	io et al. (2005)	male / 7 fema le, n=48										

M: male; F: female; NA: data not available; SCC: squamous cell carcinoma; adeno: adenocarcinoma; Gy: Gray; 5-FU: 5-fluorouracil; Ptx: paclitaxel; Cbp: Carboplatin; Cis: cisplatin; Iri: irinotecan; Oxa: oxaliplatin. \*Liver function abnormal.

6. Conclusions and Future Prospective

In cases where PET/CT indicates increased FDG activity in left liver lobes following CRT for esophageal cancer, comprehensive investigations are vital to confirm or exclude distant metastases. This ensures accurate treatment adjustment and patient management. [13] Surgery generally follows about 6–8 weeks after the end of CRT. Before proceeding to surgery, PET-CT evaluation is advised to screen for new interval metastases. These patients will usually not proceed to surgery.<sup>[10]</sup> Although post-nCRT PET is a valuable tool in assessing the response of the primary tumor to nCRT, in cases where new findings concerning for metastatic disease are detected, PET-CT often leads to a high

proportion of false positives and subsequent work-up. The work-up of false-positive post-nCRT findings includes immediate additional imaging such as high resolution CT or MRI and biopsy.<sup>[21]</sup>

**Author Contributions:** Conceptualization, S.E.S and C.I.C; methodology, S.E.S; software, Y.L.L; validation, S.E.S, C.I.C, Y.L.L and C.W.H; formal analysis, S.E.S; investigation, S.E.S; resources, Y.L.L; data curation, Y.L.L; writing—original draft preparation, S.E.S; writing—review and editing, S.E.S and Y.L.L; visualization, S.E.S; supervision, S.E.S; project administration, S.E.S; funding acquisition, S.E.S and Y.L.L..

**Funding:** This research was funded by Taichung Veterans General Hospital and National Yang-Ming University, Taichung, Taiwan, Grant No. TCVGH-YM1110105; Yen Tjing Ling Medical Foundation, Taipei, Taiwan, Grant No. CI-112-9; and Taichung Veterans General Hospital and Taichung Veterans General Hospital Chiayi Branch, Taichung, Taiwan, Grant No. TCVGH-VHCY1128602.

**Informed Consent Statement:** Patient consent was waived due to the publication as a case report in 2020.

**Acknowledgments:** Not applicable.

**Conflicts of Interest:** The authors declare no conflicts of interest.

## References

1. Pennathur, A.; Gibson, M.K.; Jobe, B.A.; Luketich, J.D. Oesophageal carcinoma. *Lancet* 2013, 381, 400-412, doi:10.1016/s0140-6736(12)60643-6.
2. Sjoquist, K.M.; Burmeister, B.H.; Smithers, B.M.; Zalcberg, J.R.; Simes, R.J.; Barbour, A.; Gebbski, V. Survival after neoadjuvant chemotherapy or chemoradiotherapy for resectable oesophageal carcinoma: an updated meta-analysis. *Lancet Oncol* 2011, 12, 681-692, doi:10.1016/s1470-2045(11)70142-5.
3. Shapiro, J.; van Lanschot, J.J.B.; Hulshof, M.; van Hagen, P.; van Berge Henegouwen, M.I.; Wijnhoven, B.P.L.; van Laarhoven, H.W.M.; Nieuwenhuijzen, G.A.P.; Hospers, G.A.P.; Bonenkamp, J.J.; et al. Neoadjuvant chemoradiotherapy plus surgery versus surgery alone for oesophageal or junctional cancer (CROSS): long-term results of a randomised controlled trial. *Lancet Oncol* 2015, 16, 1090-1098, doi:10.1016/s1470-2045(15)00040-6.
4. Daly, J.M.; Fry, W.A.; Little, A.G.; Winchester, D.P.; McKee, R.F.; Stewart, A.K.; Fremgen, A.M. Esophageal cancer: results of an American College of Surgeons Patient Care Evaluation Study. *J Am Coll Surg* 2000, 190, 562-572; discussion 572-563, doi:10.1016/s1072-7515(00)00238-6.
5. Nakahara, T.; Takagi, Y.; Takemasa, K.; Mitsui, Y.; Tsuyuki, A.; Shigematsu, N.; Kubo, A. Dose-related fluorodeoxyglucose uptake in acute radiation-induced hepatitis. *Eur J Gastroenterol Hepatol* 2008, 20, 1040-1044, doi:10.1097/MEG.0b013e3282f5f5d5.
6. Monjazeb, A.M.; Riedlinger, G.; Aklilu, M.; Geisinger, K.R.; Mishra, G.; Isom, S.; Clark, P.; Levine, E.A.; Blackstock, A.W. Outcomes of patients with esophageal cancer staged with [<sup>18</sup>F]fluorodeoxyglucose positron emission tomography (FDG-PET): can postchemoradiotherapy FDG-PET predict the utility of resection? *J Clin Oncol* 2010, 28, 4714-4721, doi:10.1200/jco.2010.30.7702.
7. Smithers, B.M.; Couper, G.C.; Thomas, J.M.; Wong, D.; Gotley, D.C.; Martin, I.; Harvey, J.A.; Thomson, D.B.; Walpole, E.T.; Watts, N.; et al. Positron emission tomography and pathological evidence of response to neoadjuvant therapy in adenocarcinoma of the esophagus. *Dis Esophagus* 2008, 21, 151-158, doi:10.1111/j.1442-2050.2007.00732.x.
8. Blom, R.L.; Schreurs, W.M.; Belgers, H.J.; Oostenbrug, L.E.; Vliegen, R.F.; Sosef, M.N. The value of post-neoadjuvant therapy PET-CT in the detection of interval metastases in esophageal carcinoma. *Eur J Surg Oncol* 2011, 37, 774-778, doi:10.1016/j.ejso.2011.06.002.
9. Bruzzi, J.F.; Munden, R.F.; Truong, M.T.; Marom, E.M.; Sabloff, B.S.; Gladish, G.W.; Iyer, R.B.; Pan, T.S.; Macapinlac, H.A.; Erasmus, J.J. PET/CT of esophageal cancer: its role in clinical management. *Radiographics* 2007, 27, 1635-1652, doi:10.1148/rq.276065742.
10. Stiekema, J.; Vermeulen, D.; Vegt, E.; Voncken, F.E.; Aleman, B.M.; Sanders, J.; Boot, H.; van Sandick, J.W. Detecting interval metastases and response assessment using 18F-FDG PET/CT after neoadjuvant chemoradiotherapy for esophageal cancer. *Clin Nucl Med* 2014, 39, 862-867, doi:10.1097/rln.0000000000000517.
11. Goense, L.; Ruurda, J.P.; Carter, B.W.; Fang, P.; Ho, L.; Meijer, G.J.; van Hillegersberg, R.; Hofstetter, W.L.; Lin, S.H. Prediction and diagnosis of interval metastasis after neoadjuvant chemoradiotherapy for oesophageal cancer using (18)F-FDG PET/CT. *Eur J Nucl Med Mol Imaging* 2018, 45, 1742-1751, doi:10.1007/s00259-018-4011-6.
12. Rabe, T.M.; Yokoo, T.; Meyer, J.; Kernstine, K.H., Sr.; Wang, D.; Khatri, G. Radiation-Induced Liver Injury Mimicking Metastatic Disease in a Patient With Esophageal Cancer: Correlation of Positron Emission Tomography/Computed Tomography With Magnetic Resonance Imaging and Literature Review. *J Comput Assist Tomogr* 2016, 40, 560-563, doi:10.1097/rct.0000000000000406.



13. Iyer, R.B.; Balachandran, A.; Bruzzi, J.F.; Johnson, V.; Macapinlac, H.A.; Munden, R.F. PET/CT and hepatic radiation injury in esophageal cancer patients. *Cancer Imaging* 2007, 7, 189-194, doi:10.1102/1470-7330.2007.0027.
14. Voncken, F.E.M.; Aleman, B.M.P.; van Dieren, J.M.; Grootsholten, C.; Lalezari, F.; van Sandick, J.W.; Steinberg, J.D.; Vegt, E. Radiation-induced liver injury mimicking liver metastases on FDG-PET-CT after chemoradiotherapy for esophageal cancer : A retrospective study and literature review. *Strahlenther Onkol* 2018, 194, 156-163, doi:10.1007/s00066-017-1217-7.
15. Reed, G.B., Jr.; Cox, A.J., Jr. The human liver after radiation injury. A form of veno-occlusive disease. *Am J Pathol* 1966, 48, 597-611.
16. Benson, R.; Madan, R.; Kilambi, R.; Chander, S. Radiation induced liver disease: A clinical update. *J Egypt Natl Canc Inst* 2016, 28, 7-11, doi:10.1016/j.jnci.2015.08.001.
17. Kim, J.; Jung, Y. Radiation-induced liver disease: current understanding and future perspectives. *Exp Mol Med* 2017, 49, e359, doi:10.1038/emm.2017.85.
18. Lawrence, T.S.; Robertson, J.M.; Anscher, M.S.; Jirtle, R.L.; Ensminger, W.D.; Fajardo, L.F. Hepatic toxicity resulting from cancer treatment. *Int J Radiat Oncol Biol Phys* 1995, 31, 1237-1248, doi:10.1016/0360-3016(94)00418-k.
19. Ogata, K.; Hizawa, K.; Yoshida, M.; Kitamuro, T.; Akagi, G.; Kagawa, K.; Fukuda, F. HEPATIC INJURY FOLLOWING IRRADIATION--A MORPHOLOGIC STUDY. *Tokushima J Exp Med* 1963, 10, 240-251.
20. Chou, C.H.; Chen, P.J.; Lee, P.H.; Cheng, A.L.; Hsu, H.C.; Cheng, J.C. Radiation-induced hepatitis B virus reactivation in liver mediated by the bystander effect from irradiated endothelial cells. *Clin Cancer Res* 2007, 13, 851-857, doi:10.1158/1078-0432.Ccr-06-2459.
21. Gabriel, E.; Alnaji, R.; Du, W.; Attwood, K.; Kukar, M.; Hochwald, S. Effectiveness of Repeat 18F-Fluorodeoxyglucose Positron Emission Tomography Computerized Tomography (PET-CT) Scan in Identifying Interval Metastases for Patients with Esophageal Cancer. *Ann Surg Oncol* 2017, 24, 1739-1746, doi:10.1245/s10434-016-5754-6.
22. Grant, M.J.; Didier, R.A.; Stevens, J.S.; Beyder, D.D.; Hunter, J.G.; Thomas, C.R.; Coakley, F.V. Radiation-induced liver disease as a mimic of liver metastases at serial PET/CT during neoadjuvant chemoradiation of distal esophageal cancer. *Abdom Imaging* 2014, 39, 963-968, doi:10.1007/s00261-014-0125-x.
23. Som, P.; Atkins, H.L.; Bandoypadhyay, D.; Fowler, J.S.; MacGregor, R.R.; Matsui, K.; Oster, Z.H.; Sacker, D.F.; Shiue, C.Y.; Turner, H.; et al. A fluorinated glucose analog, 2-fluoro-2-deoxy-D-glucose (F-18): nontoxic tracer for rapid tumor detection. *J Nucl Med* 1980, 21, 670-675.
24. Liu, Y.; Ghesani, N.V.; Zuckier, L.S. Physiology and pathophysiology of incidental findings detected on FDG-PET scintigraphy. *Semin Nucl Med* 2010, 40, 294-315, doi:10.1053/j.semnuclmed.2010.02.002.
25. von Schulthess, G.K.; Steinert, H.C.; Hany, T.F. Integrated PET/CT: current applications and future directions. *Radiology* 2006, 238, 405-422, doi:10.1148/radiol.2382041977.
26. Blodgett, T.M.; Meltzer, C.C.; Townsend, D.W. PET/CT: form and function. *Radiology* 2007, 242, 360-385, doi:10.1148/radiol.2422051113.
27. Hillner, B.E.; Siegel, B.A.; Liu, D.; Shields, A.F.; Gareen, I.F.; Hanna, L.; Stine, S.H.; Coleman, R.E. Impact of positron emission tomography/computed tomography and positron emission tomography (PET) alone on expected management of patients with cancer: initial results from the National Oncologic PET Registry. *J Clin Oncol* 2008, 26, 2155-2161, doi:10.1200/jco.2007.14.5631.
28. Poeppel, T.D.; Krause, B.J.; Heusner, T.A.; Boy, C.; Bockisch, A.; Antoch, G. PET/CT for the staging and follow-up of patients with malignancies. *Eur J Radiol* 2009, 70, 382-392, doi:10.1016/j.ejrad.2009.03.051.
29. Metser, U.; Miller, E.; Lerman, H.; Even-Sapir, E. Benign nonphysiologic lesions with increased 18F-FDG uptake on PET/CT: characterization and incidence. *AJR Am J Roentgenol* 2007, 189, 1203-1210, doi:10.2214/ajr.07.2083.
30. Beatty, J.S.; Williams, H.T.; Aldridge, B.A.; Hughes, M.P.; Vasudeva, V.S.; Gucwa, A.L.; David, G.S.; Lind, D.S.; Kruse, E.J.; McLoughlin, J.M. Incidental PET/CT findings in the cancer patient: how should they be managed? *Surgery* 2009, 146, 274-281, doi:10.1016/j.surg.2009.04.024.
31. Culverwell, A.D.; Scarsbrook, A.F.; Chowdhury, F.U. False-positive uptake on 2-[<sup>18</sup>F]-fluoro-2-deoxy-D-glucose (FDG) positron-emission tomography/computed tomography (PET/CT) in oncological imaging. *Clin Radiol* 2011, 66, 366-382, doi:10.1016/j.crad.2010.12.004.
32. Chowdhury, F.U.; Sheerin, F.; Bradley, K.M.; Gleeson, F.V. Sarcoid-like reaction to malignancy on whole-body integrated (18)F-FDG PET/CT: prevalence and disease pattern. *Clin Radiol* 2009, 64, 675-681, doi:10.1016/j.crad.2009.03.005.
33. Jacene, H.A.; Stearns, V.; Wahl, R.L. Lymphadenopathy resulting from acute hepatitis C infection mimicking metastatic breast carcinoma on FDG PET/CT. *Clin Nucl Med* 2006, 31, 379-381, doi:10.1097/01.rlu.0000222675.10765.14.
34. Ferlay, J.; Steliarova-Foucher, E.; Lortet-Tieulent, J.; Rosso, S.; Coebergh, J.W.; Comber, H.; Forman, D.; Bray, F. Cancer incidence and mortality patterns in Europe: estimates for 40 countries in 2012. *Eur J Cancer* 2013, 49, 1374-1403, doi:10.1016/j.ejca.2012.12.027.

35. Heeren, P.A.; Jager, P.L.; Bongaerts, F.; van Dullemen, H.; Sluiter, W.; Plukker, J.T. Detection of distant metastases in esophageal cancer with (18)F-FDG PET. *J Nucl Med* 2004, 45, 980-987.
36. Nijkamp, J.; Rossi, M.; Lebesque, J.; Belderbos, J.; van den Heuvel, M.; Kwint, M.; Uytendinck, W.; Vogel, W.; Sonke, J.J. Relating acute esophagitis to radiotherapy dose using FDG-PET in concurrent chemoradiotherapy for locally advanced non-small cell lung cancer. *Radiother Oncol* 2013, 106, 118-123, doi:10.1016/j.radonc.2012.09.024.
37. Ulaner, G.A.; Lyall, A. Identifying and distinguishing treatment effects and complications from malignancy at FDG PET/CT. *Radiographics* 2013, 33, 1817-1834, doi:10.1148/rg.336125105.
38. Bruzzi, J.F.; Swisher, S.G.; Truong, M.T.; Munden, R.F.; Hofstetter, W.L.; Macapinlac, H.A.; Correa, A.M.; Mawlawi, O.; Ajani, J.A.; Komaki, R.R.; et al. Detection of interval distant metastases: clinical utility of integrated CT-PET imaging in patients with esophageal carcinoma after neoadjuvant therapy. *Cancer* 2007, 109, 125-134, doi:10.1002/cncr.22397.
39. Flamen, P.; Van Cutsem, E.; Lerut, A.; Cambier, J.P.; Haustermans, K.; Bormans, G.; De Leyn, P.; Van Raemdonck, D.; De Wever, W.; Ectors, N.; et al. Positron emission tomography for assessment of the response to induction radiochemotherapy in locally advanced oesophageal cancer. *Ann Oncol* 2002, 13, 361-368, doi:10.1093/annonc/mdf081.
40. Cerfolio, R.J.; Bryant, A.S.; Ohja, B.; Bartolucci, A.A.; Eloubeidi, M.A. The accuracy of endoscopic ultrasonography with fine-needle aspiration, integrated positron emission tomography with computed tomography, and computed tomography in restaging patients with esophageal cancer after neoadjuvant chemoradiotherapy. *J Thorac Cardiovasc Surg* 2005, 129, 1232-1241, doi:10.1016/j.jtcvs.2004.12.042.
41. Weber, W.A.; Ott, K.; Becker, K.; Dittler, H.J.; Helmberger, H.; Avril, N.E.; Meisetschlager, G.; Busch, R.; Siewert, J.R.; Schwaiger, M.; et al. Prediction of response to preoperative chemotherapy in adenocarcinomas of the esophagogastric junction by metabolic imaging. *J Clin Oncol* 2001, 19, 3058-3065, doi:10.1200/jco.2001.19.12.3058.
42. Findlay, J.M.; Gillies, R.S.; Franklin, J.M.; Teoh, E.J.; Jones, G.E.; di Carlo, S.; Gleeson, F.V.; Maynard, N.D.; Bradley, K.M.; Middleton, M.R. Restaging oesophageal cancer after neoadjuvant therapy with (18)F-FDG PET-CT: identifying interval metastases and predicting incurable disease at surgery. *Eur Radiol* 2016, 26, 3519-3533, doi:10.1007/s00330-016-4227-4.
43. Levine, E.A.; Farmer, M.R.; Clark, P.; Mishra, G.; Ho, C.; Geisinger, K.R.; Melin, S.A.; Lovato, J.; Oaks, T.; Blackstock, A.W. Predictive value of 18-fluoro-deoxy-glucose-positron emission tomography (18F-FDG-PET) in the identification of responders to chemoradiation therapy for the treatment of locally advanced esophageal cancer. *Ann Surg* 2006, 243, 472-478, doi:10.1097/01.sla.0000208430.07050.61.
44. Demey, K.; Van Veer, H.; Nafteux, P.; Deroose, C.M.; Haustermans, K.; Coolen, J.; Vandecaveye, V.; Coosemans, W.; Van Cutsem, E. Hepatic radiation injury mimicking metastasis in distal esophageal cancer(). *Acta Chir Belg* 2017, 117, 250-255, doi:10.1080/00015458.2016.1248120.
45. DeLappe, E.M.; Truong, M.T.; Bruzzi, J.F.; Swisher, S.G.; Rohren, E.M. Hepatic radiation injury mimicking a metastasis on positron-emission tomography/computed tomography in a patient with esophageal carcinoma. *J Thorac Oncol* 2009, 4, 1442-1444, doi:10.1097/JTO.0b013e3181bbf208.
46. Luk, W.H.; Au-Yeung, A.W.; Loke, T.K. Imaging patterns of liver uptakes on PET scan: pearls and pitfalls. *Nucl Med Rev Cent East Eur* 2013, 16, 75-81, doi:10.5603/nmr.2013.0039.
47. Shai, S.E.; Lin, Y.H.; Lai, Y.L.; Tang, H.W.; Hsieh, Y.W.; Hung, S.C. Phantom simulation of liver metastasis on a positron emission tomography with computed tomography scan after neoadjuvant chemoradiotherapy for distal esophageal cancer: a case report. *J Med Case Rep* 2020, 14, 106, doi:10.1186/s13256-020-02391-z.
48. Pan, C.C.; Kavanagh, B.D.; Dawson, L.A.; Li, X.A.; Das, S.K.; Miften, M.; Ten Haken, R.K. Radiation-associated liver injury. *Int J Radiat Oncol Biol Phys* 2010, 76, S94-100, doi:10.1016/j.ijrobp.2009.06.092.
49. Sempoux, C.; Horsmans, Y.; Geubel, A.; Fraikin, J.; Van Beers, B.E.; Gigot, J.F.; Lerut, J.; Rahier, J. Severe radiation-induced liver disease following localized radiation therapy for biliopancreatic carcinoma: activation of hepatic stellate cells as an early event. *Hepatology* 1997, 26, 128-134, doi:10.1002/hep.510260117.
50. Fajardo, L.F.; Colby, T.V. Pathogenesis of veno-occlusive liver disease after radiation. *Arch Pathol Lab Med* 1980, 104, 584-588.
51. Dawson, L.A.; Normolle, D.; Balter, J.M.; McGinn, C.J.; Lawrence, T.S.; Ten Haken, R.K. Analysis of radiation-induced liver disease using the Lyman NTCP model. *Int J Radiat Oncol Biol Phys* 2002, 53, 810-821, doi:10.1016/s0360-3016(02)02846-8.
52. Dawson, L.A.; Ten Haken, R.K. Partial volume tolerance of the liver to radiation. *Semin Radiat Oncol* 2005, 15, 279-283, doi:10.1016/j.semradonc.2005.04.005.
53. Yamasaki, S.A.; Marn, C.S.; Francis, I.R.; Robertson, J.M.; Lawrence, T.S. High-dose localized radiation therapy for treatment of hepatic malignant tumors: CT findings and their relation to radiation hepatitis. *AJR Am J Roentgenol* 1995, 165, 79-84, doi:10.2214/ajr.165.1.7785638.

54. Munden, R.F.; Erasmus, J.J.; Smythe, W.R.; Madewell, J.E.; Forster, K.M.; Stevens, C.W. Radiation injury to the liver after intensity-modulated radiation therapy in patients with mesothelioma: an unusual CT appearance. *AJR Am J Roentgenol* 2005, 184, 1091-1095, doi:10.2214/ajr.184.4.01841091.
55. Enzinger, P.C.; Mayer, R.J. Esophageal cancer. *N Engl J Med* 2003, 349, 2241-2252, doi:10.1056/NEJMra035010.
56. Lee, U.E.; Friedman, S.L. Mechanisms of hepatic fibrogenesis. *Best Pract Res Clin Gastroenterol* 2011, 25, 195-206, doi:10.1016/j.bpg.2011.02.005.
57. Wieder, H.A.; Brücher, B.L.; Zimmermann, F.; Becker, K.; Lordick, F.; Beer, A.; Schwaiger, M.; Fink, U.; Siewert, J.R.; Stein, H.J.; et al. Time course of tumor metabolic activity during chemoradiotherapy of esophageal squamous cell carcinoma and response to treatment. *J Clin Oncol* 2004, 22, 900-908, doi:10.1200/jco.2004.07.122.
58. King, P.D.; Perry, M.C. Hepatotoxicity of chemotherapy. *Oncologist* 2001, 6, 162-176, doi:10.1634/theoncologist.6-2-162.
59. Guha, C.; Kavanagh, B.D. Hepatic radiation toxicity: avoidance and amelioration. *Semin Radiat Oncol* 2011, 21, 256-263, doi:10.1016/j.semradonc.2011.05.003.
60. Jeffrey, R.B., Jr.; Moss, A.A.; Quivey, J.M.; Federle, M.P.; Wara, W.M. CT of radiation-induced hepatic injury. *AJR Am J Roentgenol* 1980, 135, 445-448, doi:10.2214/ajr.135.3.445.
61. Unger, E.C.; Lee, J.K.; Weyman, P.J. CT and MR imaging of radiation hepatitis. *J Comput Assist Tomogr* 1987, 11, 264-268, doi:10.1097/00004728-198703000-00013.
62. Kwek, J.W.; Iyer, R.B.; Dunnington, J.; Faria, S.; Silverman, P.M. Spectrum of imaging findings in the abdomen after radiotherapy. *AJR Am J Roentgenol* 2006, 187, 1204-1211, doi:10.2214/ajr.05.0941.
63. Itai, Y.; Murata, S.; Kurosaki, Y. Straight border sign of the liver: spectrum of CT appearances and causes. *Radiographics* 1995, 15, 1089-1102, doi:10.1148/radiographics.15.5.7501852.
64. Vernuccio, F.; Cannella, R.; Bartolotta, T.V.; Galia, M.; Tang, A.; Brancatelli, G. Advances in liver US, CT, and MRI: moving toward the future. *Eur Radiol Exp* 2021, 5, 52, doi:10.1186/s41747-021-00250-0.
65. Wong, J.J.; Anthony, M.P.; Lan Khong, P. Hepatic radiation injury in distal esophageal carcinoma: a case report. *Clin Nucl Med* 2012, 37, 709-711, doi:10.1097/RLU.0b013e3182443e14.
66. Viswanathan, C.; Truong, M.T.; Sagebiel, T.L.; Bronstein, Y.; Vikram, R.; Patnana, M.; Silverman, P.M.; Bhosale, P.R. Abdominal and pelvic complications of nonoperative oncologic therapy. *Radiographics* 2014, 34, 941-961, doi:10.1148/rg.344140082.
67. Jelvehgaran, P.; Steinberg, J.D.; Khmelinskii, A.; Borst, G.; Song, J.Y.; de Wit, N.; de Bruin, D.M.; van Herk, M. Evaluation of acute esophageal radiation-induced damage using magnetic resonance imaging: a feasibility study in mice. *Radiat Oncol* 2019, 14, 188, doi:10.1186/s13014-019-1396-8.
68. Seidensticker, M.; Burak, M.; Kalinski, T.; Garlipp, B.; Koelble, K.; Wust, P.; Antweiler, K.; Seidensticker, R.; Mohnike, K.; Pech, M.; et al. Radiation-induced liver damage: correlation of histopathology with hepatobiliary magnetic resonance imaging, a feasibility study. *Cardiovasc Intervent Radiol* 2015, 38, 213-221, doi:10.1007/s00270-014-0872-7.
69. Umezawa, R.; Ota, H.; Takanami, K.; Ichinose, A.; Matsushita, H.; Saito, H.; Takase, K.; Jingu, K. MRI findings of radiation-induced myocardial damage in patients with oesophageal cancer. *Clin Radiol* 2014, 69, 1273-1279, doi:10.1016/j.crad.2014.08.010.
70. Machann, W.; Beer, M.; Breunig, M.; Störk, S.; Angermann, C.; Seufert, I.; Schwab, F.; Kölbl, O.; Flentje, M.; Vordermark, D. Cardiac magnetic resonance imaging findings in 20-year survivors of mediastinal radiotherapy for Hodgkin's disease. *Int J Radiat Oncol Biol Phys* 2011, 79, 1117-1123, doi:10.1016/j.ijrobp.2009.12.054.
71. Yankelevitz, D.F.; Henschke, C.I.; Knapp, P.H.; Nisce, L.; Yi, Y.; Cahill, P. Effect of radiation therapy on thoracic and lumbar bone marrow: evaluation with MR imaging. *AJR Am J Roentgenol* 1991, 157, 87-92, doi:10.2214/ajr.157.1.1904679.
72. Daldrup-Link, H.E.; Henning, T.; Link, T.M. MR imaging of therapy-induced changes of bone marrow. *Eur Radiol* 2007, 17, 743-761, doi:10.1007/s00330-006-0404-1.

**Disclaimer/Publisher's Note:** The statements, opinions and data contained in all publications are solely those of the individual author(s) and contributor(s) and not of MDPI and/or the editor(s). MDPI and/or the editor(s) disclaim responsibility for any injury to people or property resulting from any ideas, methods, instructions or products referred to in the content.